Available online at www.sciencedirect.com
SCIENCE DIRECT®
Superlattices and Microstructures 40 (2006) 100–112
Superlattices and Microstructures
www.elsevier.com/locate/superlattices

$\mathbf{k}\cdot\mathbf{p}$ calculations for double p-type δ-doped quantum wells in GaAs

Isaac Rodríguez-Vargas*, Miguel E. Mora-Ramos[1]

Facultad de Ciencias, Universidad Autónoma del Estado de Morelos, Av. Universidad 1001, Col. Chamilpa, 62210 Cuernavaca, MOR., Mexico

Received 6 February 2006; received in revised form 11 May 2006; accepted 16 May 2006
Available online 11 July 2006

Abstract

The hole subband structure in double p-type δ-doped quantum wells in GaAs is computed with the use of the 4×4 $\mathbf{k}\cdot\mathbf{p}$ Hamiltonian. The Thomas–Fermi–Dirac approach is implemented for the description of the valence band bending, and the hole states at the Brillouin zone center are calculated along its lines, within the effective mass approximation. The zone center eigenstates obtained are then used to diagonalize the $\mathbf{k}\cdot\mathbf{p}$ Hamiltonian for non-zero $\mathbf{k}$. The hole subband structure is analyzed as a function of the impurity density and the distance between δ wells.

Keywords: Hole subband structure; Double δ-doped quantum wells; $\mathbf{k}\cdot\mathbf{p}$ approximation

1. Introduction

The advancement in growth and doping techniques allows the fabrication of semiconducting structures with very sharp doping profiles within a few atomic layers: the so-called δ-doping. Systems bearing δ-doped profiles are of interest for basic research as well as for possible device applications (see, for instance, [1,2], and references therein). In particular, p-type δ-doped quantum wells have played a fundamental role in the fabrication of diamond-based field effect transistors with outstanding characteristics [3,4].

* Corresponding author. Tel.: +52 777 329 7020; fax: +52 777 329 7040.
E-mail address: irv@buzon.uaem.mx (I. Rodríguez-Vargas).
[1] Currently on sabbatical leave at the Instituto de Ciencia de Materiales de Madrid, 28049, Cantoblanco, Madrid, Spain.

0749-6036/$ - see front matter
doi:10.1016/j.spmi.2006.05.006

From the theoretical point of view single δ-doped (*SDD*) wells in GaAs have been quite extensively studied [5–22]. However, much less work on double δ-doped (*DDD*) QW's in GaAs has been reported [23–27]. The *DDD* structures offer an improvement in the transport properties with respect to the *SDD* ones [28–32]. This improvement is of importance for possible implementation in high speed, amplifier, and switching devices, in which a high density charge – and consequently, mobility – is sought. On the other hand, diamond-based stacked p–delta-doped structures have shown promising features as vertical power diodes with very good on-resistance to blocking voltage ratio [33].

Due to those properties, a more complete and rigorous calculation of the hole subband structure of multiple p–delta-doped systems is necessary to understand the underlying physics behind these layered systems. In the present work we limit ourselves to study the hole subband structure of the two-dimensional hole gas in the GaAs *DDD* QW. The band bending profile is described analytically along the lines of the local density Thomas–Fermi–Dirac (TFD) approximation, including the exchange contribution [26]. With the derived model potential we have calculated the eigenstates and eigenfunctions at the Brillouin zone center. Then, this set of eigenstates are taken as a basis for the diagonalization of the 4×4 $\mathbf{k}\cdot\mathbf{p}$ Hamiltonian, thus obtaining the hole subband structure for $k \neq 0$, which is analyzed as a function of the doping density and the interwell distance.

2. Method and model

For a single δ-doped quantum well, a direct relation between the density $p(z)$ and the Hartree potential $V_H(z)$ was previously obtained in the one-dimensional TFD approach within the local density approximation (LDA) [17]. It is written as

$$p_{au}(z) = \frac{m_a^3 \varsigma^3(w)}{3\pi^5}\left[1 - \sqrt{1 + \frac{\pi^2(\mu^* - V_H^*(z))}{\varsigma^2(w) m_a}}\right]^3, \tag{1}$$

where $V_H^* = V_H/R_y^*$, $\mu^* = \mu/R_y^*$, $m_a = \left[1 + \left(\frac{m_{lh}}{m_{hh}}\right)^{3/2}\right]^{2/3}$, where m_{hh} and m_{lh} are the heavy and light hole masses, respectively. $\varsigma(w)$ accounts for the valence band coupling and is given by [34]

$$\varsigma(w) = 2^{-1/3} + (1 - w^2)[w^2(aw + b) + c(4w^3 + 3w^2 + 2w + 1)], \tag{2}$$

where $w = \sqrt{m_{lh}/m_{hh}}$, $a = 0.679$, $b = -0.0686$ and $c = -0.0811$. By including Eq. (1) in the corresponding Poisson equation, an explicit expression for the Hartree potential centered in $z = d$ is obtained. It has the form

$$V_H^*(z) - \mu^* = -\frac{\alpha^2}{(\alpha\,|z - d| + z_0)^4}, \tag{3}$$

with $\alpha = \frac{2m_a^{3/2}}{15\pi}$ and $z_0 = \left(\frac{\alpha^3}{\pi p_{2D}}\right)^{1/5}$ (effective heavy-hole-related $GaAs$ atomic units are used throughout).

In the framework of the LDA, the exchange potential for a hole gas can be written as

$$V_x^*(z) = -\varsigma(w)\frac{2}{\pi}(3\pi^2)^{1/3}(p_{au}(z))^{1/3}. \tag{4}$$

Using the relation between $p_{au}(z)$ and $V_H(z)$ it is possible to write the total potential $V^* = V_H^* + V_x^*$ as

$$V^*(z) = -\frac{\alpha^2}{(\alpha\,|z-d|+z_0)^4} - \frac{2\varsigma^2(w)m_a}{\pi^2}\left[1-\sqrt{1+\frac{\pi^2}{\varsigma^2(w)m_a}\frac{\alpha^2}{(\alpha\,|z-d|+z_0)^4}}\right]. \tag{5}$$

The latter equation summarizes the model for the band bending profile. Instead of carrying out numerically troublesome self-consistent calculations, we simply solve two Schrödinger-like effective mass equations at the zone center $\mathbf{k} = \mathbf{0}$, thus obtaining the corresponding ladders of the hole levels.

The construction of a model potential for the *DDD* is performed via an appropriate combination of two single δ-wells centered at $z = -l/2$ and $z = l/2$, considering the same impurity density in both doping spikes, as has been reported in [26]. Again, the solutions of effective mass Schrödinger equations lead to the Brillouin zone center states for both heavy and light holes.

The next step is the diagonalization of the 4×4 $\mathbf{k}\cdot\mathbf{p}$ Luttinger–Kohn Hamiltonian [36]. That is, we need to solve the secular problem

$$\begin{pmatrix} H^{hh} & b & c & 0 \\ b^* & H^{lh} & 0 & c \\ c^* & 0 & H^{lh} & -b \\ 0 & c^* & -b^* & H^{hh} \end{pmatrix} \begin{pmatrix} \phi_m^{3/2,3/2}(\vec{\kappa},z) \\ \phi_m^{3/2,1/2}(\vec{\kappa},z) \\ \phi_m^{3/2,-1/2}(\vec{\kappa},z) \\ \phi_m^{3/2,-3/2}(\vec{\kappa},z) \end{pmatrix} = E^h(\vec{k}) \begin{pmatrix} \phi_m^{3/2,3/2}(\vec{\kappa},z) \\ \phi_m^{3/2,1/2}(\vec{\kappa},z) \\ \phi_m^{3/2,-1/2}(\vec{\kappa},z) \\ \phi_m^{3/2,-3/2}(\vec{\kappa},z) \end{pmatrix} \tag{6}$$

where $\phi_m^{\nu}(\vec{\kappa},z)$ is the function associated with the confining potential of the quantum wells. The components with $\nu = 3/2, \pm 3/2$ and $\nu = 3/2, \pm 1/2$ correspond to the heavy and light holes, respectively. m is the subband index and $E^h(\vec{\kappa})$ are the energy eigenvalues of the holes. In effective atomic units, the matrix elements in Eq. (6) are given by

$$\begin{aligned} H^{hh} &= -\left[\eta_1\kappa^2 + \frac{\partial^2}{\partial z^2}\right] + V(z), \\ H^{lh} &= -\left[\eta_2\kappa^2 + \xi_1\frac{\partial^2}{\partial z^2}\right] + V(z), \\ b &= -6\,i\,\xi_3\,(\sin\theta+\cos\theta)\,\kappa\,\frac{\partial}{\partial z}, \\ c &= 6\,i\,(\xi_2\cos^2 2\theta - i\xi_3\sin^2 2\theta)\,\kappa^2 \end{aligned} \tag{7}$$

with

$$\eta_1 = \frac{\gamma_1+\gamma_2}{\gamma_1-2\gamma_2}, \qquad \eta_2 = \frac{\gamma_1-\gamma_2}{\gamma_1-2\gamma_2},$$
$$\xi_1 = \frac{\gamma_1+2\gamma_2}{\gamma_1-2\gamma_2}, \qquad \xi_2 = \frac{\gamma_2}{\gamma_1-2\gamma_2}, \qquad \xi_3 = \frac{\gamma_3}{\gamma_1-2\gamma_2}.$$

Here, γ_1, γ_2 and γ_3 are the Luttinger parameters, $\vec{\kappa} = (\kappa_x, \kappa_y)$ is the parallel wavevector in the x–y plane of the well, θ is the angle between $\vec{\kappa}$ and the κ_x-direction. $V(z)$ represents the confinement potential, which in our case is given by Eq. (5).

The technique chosen for this process consists in the use of the set of Γ-point wavefunctions as a basis for the expansion of the non-Γ-point states. Mathematically this reads as follows: At

the Γ point, $\kappa_x = \kappa_y = 0$, $E^h(\vec{\kappa}) = E_0^h(k_z)$. At the same time, there is no interband coupling ($b = c \equiv 0$). Eq. (7) is simplified to

$$\begin{aligned} H^{hh} &= -\frac{\partial^2}{\partial z^2} + V(z) \\ H^{lh} &= -\xi_1 \frac{\partial^2}{\partial z^2} + V(z). \end{aligned} \tag{8}$$

We can also write $\xi_1 = m_{hh}/m_{lh}$ provided that the effective masses of the heavy and light holes are defined as $m_{hh} = m_0/(\gamma_1 - 2\gamma_2)$ and $m_{lh} = m_0/(\gamma_1 + 2\gamma_2)$, respectively. In consequence Eq. (6) is reduced to two independent effective mass Schrödinger equations with eigenvalues E_0^{hh}, and E_0^{lh}, and eigenfunctions $\phi_{0m}^{3/2,\pm 3/2}(z)$, and $\phi_{0m}^{3/2,\pm 1/2}(z)$, for heavy and light holes respectively.

At the Γ point the heavy hole states $\phi_{0m}^{3/2,3/2}$ and $\phi_{0m}^{3/2,-3/2}$ are degenerate and have the same quantized energies E_{0m}^{hh}. The same happens between $\phi_{0m}^{3/2,1/2}$ and $\phi_{0m}^{3/2,-1/2}$ with quantized energies E_{0m}^{lh}. If the spin is not considered, $\phi_{0m}^{3/2,3/2}$ and $\phi_{0m}^{3/2,-3/2}$ are in fact the same solution, and so are $\phi_{0m}^{3/2,1/2}$ and $\phi_{0m}^{3/2,-1/2}$.

Now for $\kappa_x, \kappa_y \neq 0$, and $b, c \neq 0$, effects of mixing between the heavy and light hole bands exist. In order to solve the Luttinger–Kohn equation, Eq. (6), and obtain the hole eigenvalues and eigenfunctions at non-Γ points we take a basis for the energy representation that consists of the above eigenstates $\phi_{0m}^{v}(z)$ at Γ point. Then, it is proposed that the eigenfunctions sought, $\phi_m^v(\vec{\kappa}, z)$, can be expanded as

$$\begin{aligned} \phi_m^{3/2,3/2} &= \sum_{l=1}^{n1} A_l \phi_{0l}^{3/2,3/2} \quad \phi_m^{3/2,1/2} = \sum_{l=1}^{n2} B_l \phi_{0l}^{3/2,1/2} \\ \phi_m^{3/2,-1/2} &= \sum_{l=1}^{n2} C_l \phi_{0l}^{3/2,-1/2} \quad \phi_m^{3/2,-3/2} = \sum_{l=1}^{n1} D_l \phi_{0l}^{3/2,-3/2} \end{aligned} \tag{9}$$

where n_1 and n_2 are the numbers of energy eigenfunctions $\phi_{0l}^{3/2,\pm 3/2}$ and $\phi_{0l}^{3/2,\pm 1/2}$ at the Γ point, respectively. A_l, B_l, C_l and D_l are the expanding coefficients. Multiplying Eq. (6) by the matrix $\left[\phi_m^{*3/23/2}, \phi_m^{*3/21/2}, \phi_m^{*3/2-1/2}, \phi_m^{*3/2-3/2}\right]$ and substituting Eq. (9) into the result, and then integrating over z, it is possible to obtain the following energy matrix equation [37]:

$$\begin{pmatrix} \mathbf{H^{hh}} & \mathbf{b} & \mathbf{c} & \mathbf{0'} \\ \mathbf{b}^\dagger & \mathbf{H^{lh}} & \mathbf{0''} & \mathbf{c} \\ \mathbf{c}^\dagger & \mathbf{0''} & \mathbf{H^{lh}} & -\mathbf{b} \\ \mathbf{0'} & \mathbf{c}^\dagger & -\mathbf{b}^\dagger & \mathbf{H^{hh}} \end{pmatrix} \begin{pmatrix} \mathbf{A} \\ \mathbf{B} \\ \mathbf{C} \\ \mathbf{D} \end{pmatrix} = E^h \begin{pmatrix} \mathbf{A} \\ \mathbf{B} \\ \mathbf{C} \\ \mathbf{D} \end{pmatrix} \tag{10}$$

where $\mathbf{0'}$ and $\mathbf{0''}$ are the zero square matrices of n_1 and n_2 orders, respectively. The energy eigenvectors $\mathbf{A}$, $\mathbf{B}$, $\mathbf{C}$ and $\mathbf{D}$ are given by

$$\mathbf{A} = \begin{pmatrix} A_1 \\ A_2 \\ \vdots \\ A_{n_1} \end{pmatrix} \quad \mathbf{B} = \begin{pmatrix} B_1 \\ B_2 \\ \vdots \\ B_{n_2} \end{pmatrix} \quad \mathbf{C} = \begin{pmatrix} C_1 \\ C_2 \\ \vdots \\ C_{n_2} \end{pmatrix} \quad \mathbf{D} = \begin{pmatrix} D_1 \\ D_2 \\ \vdots \\ D_{n_1} \end{pmatrix} \tag{11}$$

and the matrix elements of Eq. (10) emerge as

$$
\begin{aligned}
H_{l'l}^{hh} &= \int_{-\infty}^{\infty} \phi_{0l'}^{*3/,23/2} H^{hh} \phi_{0l}^{3/2,3/2} \mathrm{d}z \qquad (l', l = 1, 2, \ldots, n_1) \\
H_{l'l}^{lh} &= \int_{-\infty}^{\infty} \phi_{0l'}^{*3/2,1/2} H^{lh} \phi_{0l}^{3/2,1/2} \mathrm{d}z \qquad (l', l = 1, 2, \cdots, n_2) \\
b_{l'l} &= \int_{-\infty}^{\infty} \phi_{0l'}^{*3/2,3/2} b \phi_{0l}^{3/2,1/2} \mathrm{d}z \qquad (l' = 1, 2, \ldots, n_1, l = 1, 2, \ldots, n_2) \\
c_{l'l} &= \int_{-\infty}^{\infty} \phi_{0l'}^{*3/2,3/2} c \phi_{0l}^{3/2,1/2} \mathrm{d}z \qquad (l' = 1, 2, \ldots, n_1, l = 1, 2, \ldots, n_2).
\end{aligned}
\tag{12}
$$

The computation of the coefficient matrix in Eq. (10) is needed to obtain the quantized energy values E_m^{hh} and $E_{m'}^{lh}$ as well as their corresponding relative energy eigenvectors **A**, **B**, **C** and **D** for heavy and light holes at the non-Γ states.

The above described method has been previously applied to the obtaining of the hole structure in strained multiple quantum wells [37] and in diamond δ-doped systems [38–41].

3. Results and discussion

The input parameters for the p-type delta quantum wells are: $\gamma_1 = 7.0$, $\gamma_2 = 2.25$, $\gamma_3 = 8.2$ [35], $\epsilon_r = 12.5$ and $1 \times 10^{12} \leq p_{2D} \leq 1 \times 10^{13}$ cm^{-2}.

In Fig. 1 the potential profile and wavefunctions of the single δ-doped quantum wells are depicted for two impurity densities, $p_{2D} = 3 \times 10^{12}$ cm^{-2} (a) and $p_{2D} = 5 \times 10^{12}$ cm^{-2} (b). It is seen that the main difference between these figures is in the depth of the potential profile. This is reflected in the number of confined states, which is a situation typical of the δ-doped systems. The hole subband structure of the above mentioned densities is presented as a function of the wavevector $\vec{\kappa}$, in Figs. 2 and 3 for the directions [10] (a) and [11] (b) of the two-dimensional Brillouin zone (in fact, corresponding to directions [100] and [110] of the crystal 3D zone). In both structures the intersubband interaction takes place between the ground heavy hole (hh) subband and the ground light hole (lh) one. The subband mixing becomes stronger for higher impurity density.

For the case of *DDD* quantum wells Fig. 4 shows the potential profile and the wavefunctions for two different impurity densities, $p_{2D} = 3 \times 10^{12}$ cm^{-2} (a) and $p_{2D} = 5 \times 10^{12}$ cm^{-2} (b), keeping the interwell distance fixed, $l = 60$ Å. The eigenfunctions presented in Fig. 4 have been computed at the zone center, $\mathbf{k} = \mathbf{0}$. Again, as long as the impurity density increases the δ wells become deeper. Consequently the number of levels confined into the wells increases. The same effect occurs when the interwell distance enlarges, while the impurity concentration remains fixed; $p_{2D} = 4 \times 10^{12}$ cm^{-2}, Fig. 5. This happens because the screening length is much bigger than the distance between wells, and when they are separating the system resembles a single well. The difference here is that the well width increases and – as a consequence – more levels localize. That behavior gradually disappears, for the influence of the potential barrier is strengthened as long as the interwell separation augments, in such a way that the energy level structure of the isolated single delta quantum well is attained.

In Fig. 6 we present the hole subband structure in the directions [100] (a) and [110] (b), with $l = 20$ Å and $p_{2D} = 3 \times 10^{12}$ cm^{-2}. We have found three subbands, two corresponding to the heavy holes and one to the light holes. A strong interaction between the ground hh and lh subbands is present in both directions. On increasing the distance between wells to 80 Å it

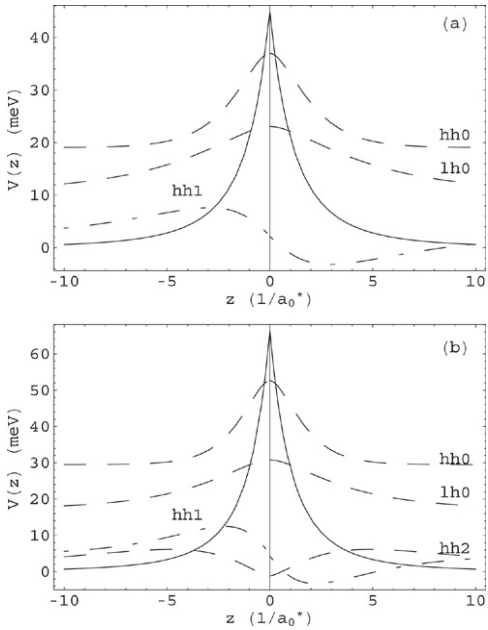

Fig. 1. Potential profile and eigenfunctions of *SDD* QW's with $p_{2D} = 3.0 \times 10^{12}$ cm^{-2} (a) and $p_{2D} = 5.0 \times 10^{12}$ cm^{-2} (b). Conventional units have been restored in the vertical axis.

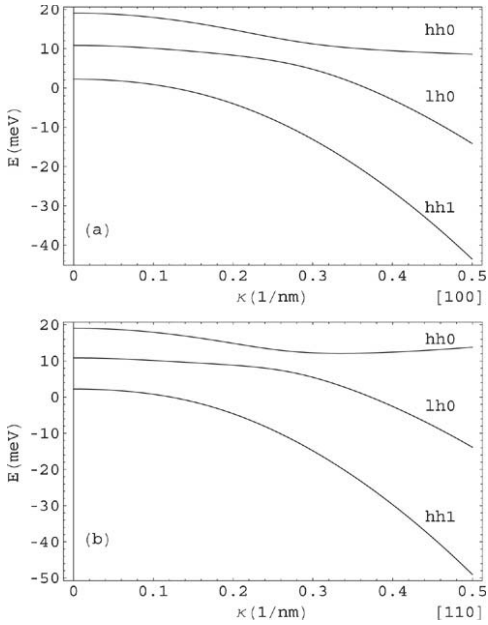

Fig. 2. The hole subband structure of *SDD* QW's in the directions [100] (a), and [110] (b), with $p_{2D} = 3.0 \times 10^{12}$ cm^{-2}. As usual, energies are represented on the vertical axis while the horizontal one contains the values of the 2D wavevector κ. Conventional units have been restored.

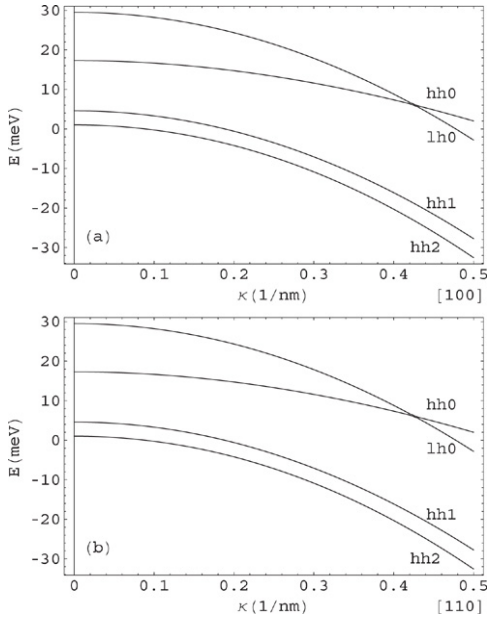

Fig. 3. The hole subband structure of *SDD* QW's in the directions [100] (a), and [110] (b), with $p_{2D} = 5.0 \times 10^{12}$ cm^{-2}.

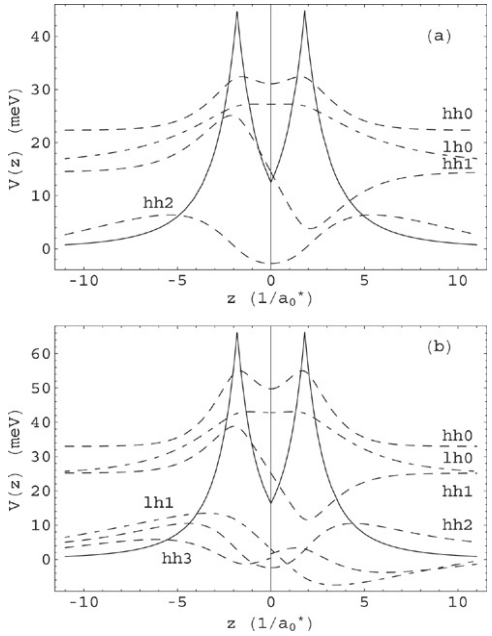

Fig. 4. Potential profile and eigenfunctions of *DDD* QW's for $p_{2D} = 3.0 \times 10^{12}$ cm^{-2} (a) and $p_{2D} = 5 \times 10^{12}$ cm^{-2} (b), and $l = 60$ Å in both cases. The wavefunctions have been computed at the zone center.

is observed that the first excited *hh* subband is closer to the ground *lh* subband due to the higher attractiveness of the δ-doped wells. As a consequence the *lh* subband presents a strong

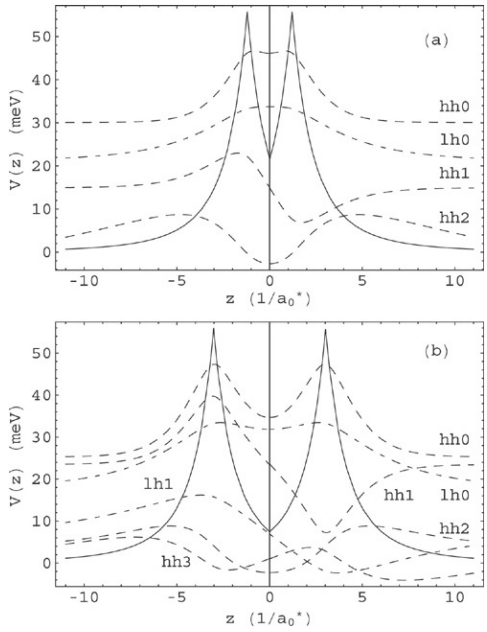

Fig. 5. Potential profile and eigenfunctions of *DDD* QW's for $l = 40$ Å (a), $l = 120$ Å (b), and $p_{2D} = 4.0 \times 10^{12}$ cm^{-2} in both cases. The wavefunctions have been computed at the zone center.

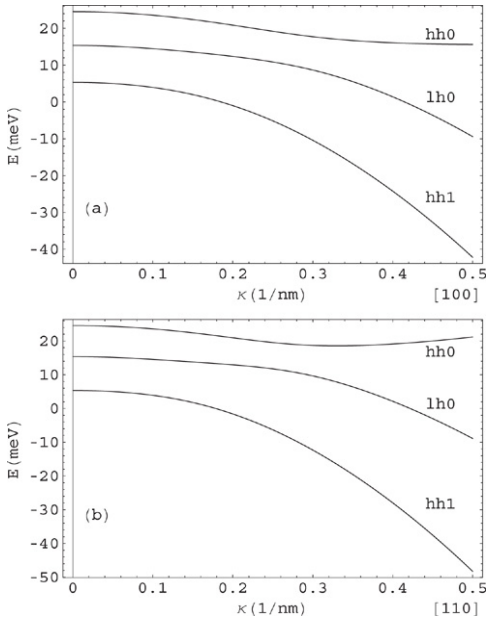

Fig. 6. The hole subband structure of *DDD* QW's in the directions [100] (a), and [110] (b), with $l = 20$ Å and $p_{2D} = 3.0 \times 10^{12}$ cm^{-2}.

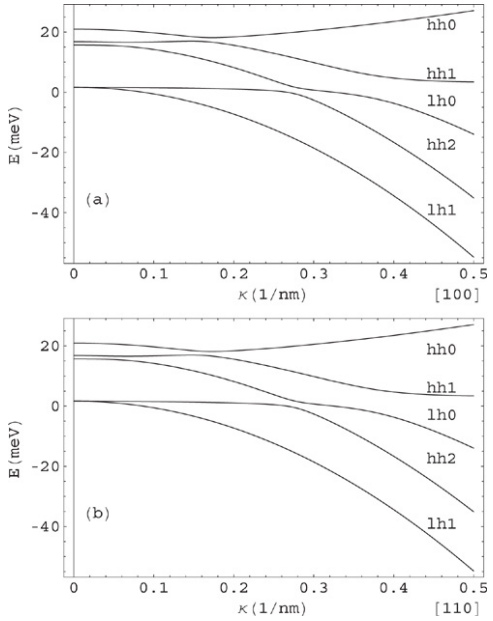

Fig. 7. The hole subband structure of *DDD* QW's in the directions [100] (a), and [110] (b), with $l = 80$ Å and $p_{2D} = 3.0 \times 10^{12}$ cm^{-2}.

interaction with the first excited hh subband as well as with the ground hh subband; Fig. 7. A further increase in the interwell distance up to 140 Å gives five subbands, three corresponding to hh and two to lh; Fig. 8. The ground and first excited hh subbands are almost degenerate, and an important interaction between the first excited hh subband and the ground lh subband is visible.

To analyze the hole subband structure as a function of the impurity density we have considered an acceptor concentration $p_{2D} = 5 \times 10^{12}$ cm^{-2}. The same interwell distances are taken into account; $l = 20$ Å, $l = 80$ Å, and $l = 140$ Å (Figs. 9–11, respectively). As we have mentioned, an increase in the impurity density brings about an increase in the potential depth and therefore leads to a more effective confinement. This is reflected in the number of confined subbands, from three in the case of Fig. 6 to four in the case of Fig. 9. In the case of Fig. 10 the number of subbands is six, while Fig. 7 presents five. There is also evident a strong interaction between all subbands. In the case of Fig. 11 the subbands are also six, and the ground and first excited hh subbands are close to degeneracy. A strong interaction between the hh and lh subbands can be seen.

In general, the change in the direction within the two-dimensional Brillouin zone causes only small differences in position of the mixing points and in the energy values of the different subbands. This seems to be a property of GaAs p–delta-doped systems. In other materials – such as diamond – the choosing of different directions in **k**-space allows one to identify more significant differences [39–41].

Another aspect worth noticing is that the interaction between the first and second subbands leads to an "anomalous" dispersion of the ground state beyond the mixing point in the near zone center region. It is seen that this inflexion is more pronounced in the case of lower impurity densities. When the impurity density is larger, the inflexion is less pronounced and occurs for

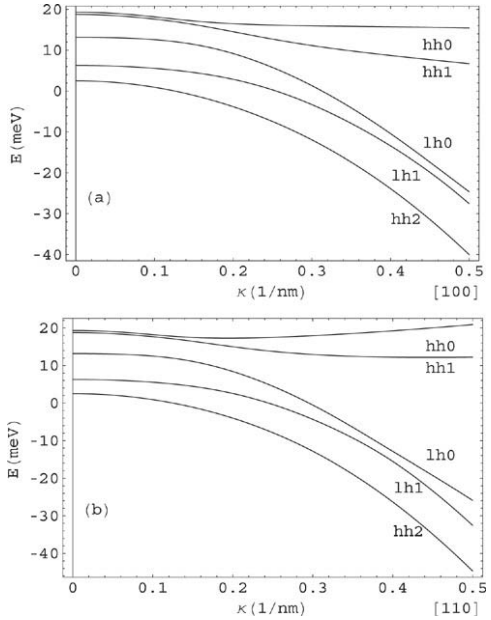

Fig. 8. The hole subband structure of *DDD* QW's in the directions [100] (a), and [110] (b), with $l = 140$ Å and $p_{2D} = 3.0 \times 10^{12}$ cm^{-2}.

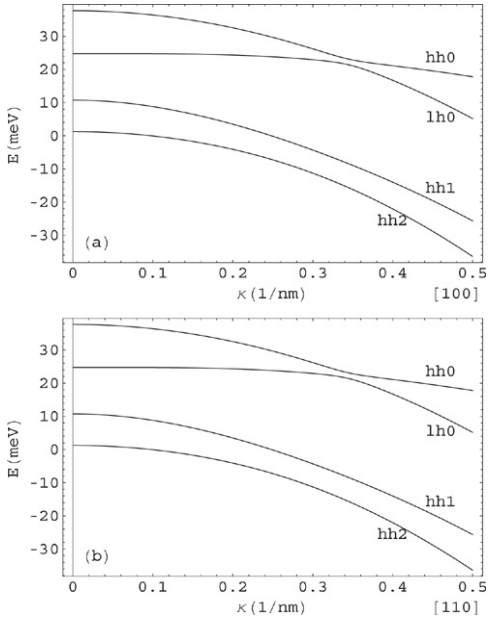

Fig. 9. The hole subband structure of *DDD* QW's in the directions [100] (a), and [110] (b), with $l = 20$ Å and $p_{2D} = 5.0 \times 10^{12}$ cm^{-2}.

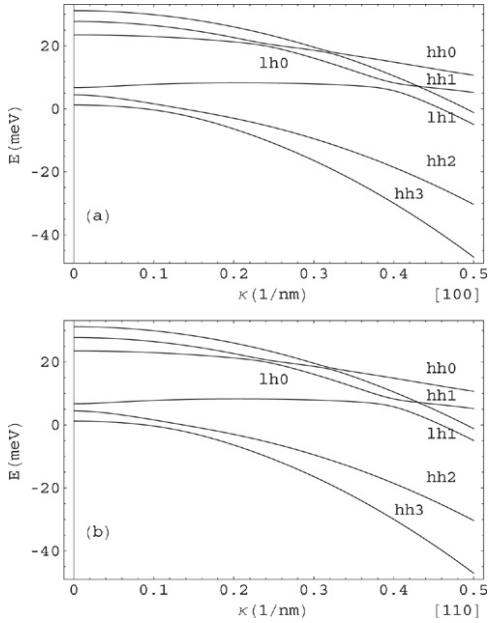

Fig. 10. The hole subband structure of *DDD* QW's in the directions [100] (a), and [110] (b), with $l = 80$ Å and $p_{2D} = 5.0 \times 10^{12}$ cm^{-2}.

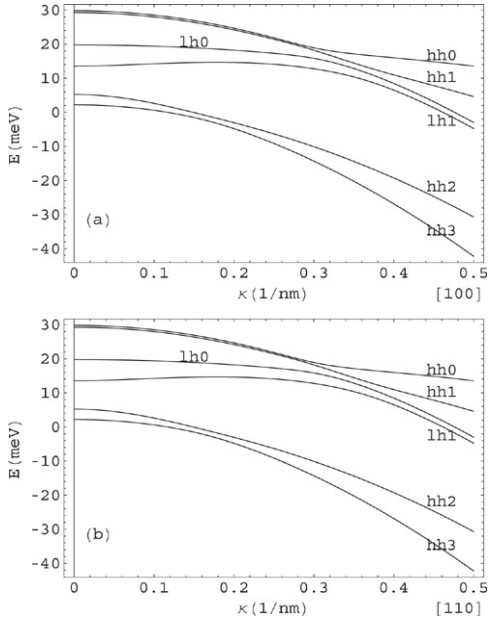

Fig. 11. The hole subband structure of *DDD* QW's in the directions [100] (a), and [110] (b), with $l = 140$ Å and $p_{2D} = 5.0 \times 10^{12}$ cm^{-2}.

Table 1
Hole subband energies (E_{hh0}, E_{lh0}, E_{hh1}, etc.) at the zone center for different distances between δ-wells and impurity densities

l	$p_{2D} = 3 \times 10^{12}$ cm^{-2} $V_0 = 44.89$ meV					$p_{2D} = 5 \times 10^{12}$ cm^{-2} $V_0 = 66.34$ meV					
	E_{hh0}	E_{lh0}	E_{hh1}	E_{hh2}	E_{lh1}	E_{hh0}	E_{lh0}	E_{hh1}	E_{hh2}	E_{lh1}	E_{hh3}
0	19.05	10.84	2.23			29.50	17.03	4.60	1.02		
20	24.55	15.41	5.37			37.71	24.74	10.75	1.60		
40	24.01	16.69	10.37			35.80	25.03	19.59	2.39		
60	22.34	16.44	14.46	1.28		32.99	25.01	25.19	3.47	3.02	1.02
80	21.00	15.60	16.80	1.54		31.18	23.48	27.74	4.46	6.73	1.23
100	20.95	15.68	16.81	1.72	1.60	30.26	22.03	28.74	5.02	9.86	1.64
120	19.56	13.91	18.54	2.35	4.95	29.97	20.81	29.10	5.37	12.18	2.13
140	19.32	13.17	18.78	2.51	6.29	29.82	19.77	29.27	5.24	13.55	2.21

The potential depth (V_0) is also indicated for the corresponding impurity density. The energies, distances and densities are in meV, Å and cm^{-2}, respectively.

higher values of the two-dimensional wavenumber; thus the parabolic model for the near zone center region might work better. Although the intersubband interactions give rise to the mixing of higher states as well, the main changes in the dispersion curves are detected for the lower ones, because they interact more strongly.

In Table 1 the hole subband energies at the zone center for $p_{2D} = 3 \times 10^{12}$ cm^{-2} and $p_{2D} = 5 \times 10^{12}$ cm^{-2} are presented as a function of the interwell distance from 0 to 140 Å with a step of 20 Å. The case $l = 0$ Å is a reference and corresponds to a *SDD* with the same impurity density as one well in the *DDD* system. We also present the potential depth for both densities.

4. Conclusions

The use of approximate TF-type models for the description of hole energies in double GaAs p-type delta-doped quantum wells has been restricted to deal with zone center states. Previous findings have allowed us to establish that a Thomas–Fermi–Dirac approach leads to a better description of the hole level ladders for $\kappa = 0$ [17,26]. The results of the present work go beyond, by extending such treatment to non-Γ states, and show how the heavy and light hole subband spectra are affected by the interband interaction for states with two-dimensional wavevector close to the Γ point. This modification could be of importance for the optical properties associated with intersubband transitions. In this sense, the description of the hole energy structure is more complete. We believe that within the chosen approximation our procedure may provide a quite accurate and simple alternative for calculation.

It is shown in this work that the interaction between subbands in the *DDD* quantum wells is important and that the assumption of parabolic bands may not be fulfilled, even close to the zone center. The *DDD* system is more complex, and presents a variety of possibilities depending on the distances between wells and the impurity content in the δ-doped planes in comparison to the *SDD* quantum wells.

Acknowledgement

M.E. Mora-Ramos acknowledges assistance for the completion of this work from the Ministerio de Educacion y Ciencia of Spain under Sabbatical Fellowship SAB2004-0199.

References

[1] L.M. Gaggero-Sager, R. Perez-Alvarez, J. Appl. Phys. 78 (1995) 4566.
[2] J.C. Martinez-Orozco, L.M. Gaggero-Sager, S.J. Vlaev, Mater. Sci. Eng. B 84 (2001) 155.
[3] A. Aleksov, A. Vescan, M. Kunze, P. Glucher, W. Ebert, E. Kohn, A. Bergmaier, G. Dollinger, Diam. Relat. Mater. 8 (1999) 941.
[4] A. Aleksov, A. Denisenko, M. Kunze, A. Vescan, A. Bergmaier, G. Dollinger, W. Ebert, E. Kohn, Semicond. Sci. Technol. 18 (2003) S59.
[5] A. Zrenner, F. Koch, K. Ploog, Surf. Sci. 196 (1988) 671.
[6] M. Santos, T. Sajoto, A. Zrenner, M. Shayegan, Appl. Phys. Lett. 53 (1988) 2504.
[7] L. Ioriatti, Phys. Rev. B 41 (1990) 8340.
[8] M.H. Degani, J. Appl. Phys. 70 (1991) 4362.
[9] S.M. Shibli, L.M.R. Scolfaro, J.R. Leitte, C.A.C. Mendoca, F. Plentz, E.A. Meneses, Appl. Phys. Lett. 60 (1992) 2895.
[10] L. Chico, F. Garcia-Moliner, V.R. Velasco, Phys. Rev. B 48 (1993) 11 427.
[11] G.-Q. Hai, N. Studart, F.M. Peeters, Phys. Rev. B 52 (1995) 8363.
[12] D. Richards, J. Wagner, H. Schneider, G. Hensdorfer, H. Maier, A. Fischer, K. Ploog, Phys. Rev. B 47 (1993) 9629.
[13] L.M. Gaggero-Sager, R. Perez-Alvarez, J. Appl. Phys. 79 (1995) 3351.
[14] G.M. Sipahi, R. Enderlein, L.M.R. Scolfaro, J.R. Leite, Phys. Rev. B 53 (1996) 9930.
[15] L.M. Gaggero-Sager, M.E. Mora-Ramos, D.A. Contreras-Solorio, Phys. Rev. B 57 (1998) 6286.
[16] S.J. Vlaev, L.M. Gaggero-Sager, Phys. Rev. B 58 (1998) 1142.
[17] L.M. Gaggero-Sager, Phys. Status Solidi b 231 (2002) 243.
[18] E. Ozturk, Y. Ergun, H. Sari, I. Sokmen, J. Appl. Phys. 91 (2002) 2118.
[19] E. Ozturk, I. Sokmen, J. Phys. D 36 (2003) 2457.
[20] J. Osvald, Physica E 23 (2004) 147.
[21] J. Osvald, J. Phys. D 37 (2004) 2655.
[22] E. Ozturk, H. Sari, Y. Ergun, I. Sokmen, Appl. Phys. A 80 (2005) 167.
[23] P.M. Koenraad, A.C.L. Heessels, F.A.P. Blom, J.A.A.J. Perenboom, J.H. Wolter, Physica B 184 (1993) 221.
[24] G.-Q. Hai, N. Studart, F.M. Peeters, Phys. Rev. B 52 (1995) 11273.
[25] E. Ozturk, Y. Ergun, H. Sari, I. Sokmen, Appl. Phys. A 77 (2003) 427.
[26] I. Rodriguez-Vargas, L.M. Gaggero-Sager, V.R. Velasco, Surf. Sci. 537 (2003) 75.
[27] E. Ozturk, I. Sokmen, Superlatt. Microstruct. 35 (2004) 95.
[28] X. Zheng, T.K. Carns, K.L. Wang, B. Wu, Appl. Phys. Lett. 62 (1993) 504.
[29] H.M. Shieh, W.C. Hsu, C.L. Wu, Appl. Phys. Lett. 63 (1993) 509.
[30] C.L. Wu, W.C. Hsu, H.M. Shieh, W.C. Liu, Appl. Phys. Lett. 64 (1994) 3027.
[31] H.-M. Sheih, C.-L. Wu, W.-C. Hsu, Y.-H. Wu, M.-J. Kao, Jpn. J. Appl. Phys. 33 (1994) 1778.
[32] V.L. Gurtovoi, V.V. Valyaev, S.Yu. Shapoval, A.N. Pustovit, Appl. Phys. Lett. 72 (1998) 1202.
[33] A. Denisenko, E. Kohn, Diam. Relat. Mater. 14 (2005) 491.
[34] P.A. Bobbert, H. Wieldraaijer, R. van der Weide, M. Kemerink, P.M. Koenraad, J.H. Wolter, Phys. Rev. B. 56 (1997) 3664; M. Combescot, P. Nozieres, J. Phys. C 5 (1972) 2369.
[35] P.Y. Yu, M. Cardona, Fundamental of Semiconductors, 2nd ed., Springer, Berlin, 1999.
[36] J.M. Luttinger, W. Kohn, Phys. Rev. 97 (1955) 869.
[37] C.S. Ma, C.H. Han, S.Y. Liu, Opt. Quantum Electron. 29 (1997) 697.
[38] M.E. Mora-Ramos, Phys. Status Solidi b 234 (2002) 481; Phys. Status Solidi b 240 (2003) 663.
[39] M.E. Mora-Ramos, Diam. Relat. Mater. 12 (2003) 33.
[40] M.E. Mora-Ramos, Diam. Relat. Mater. 12 (2003) 550.
[41] M.E. Mora-Ramos, Diam. Relat. Mater. 12 (2003) 1653; Diam. Relat. Mater. 13 (2004) 539.